Memoirs of the Faculty of Engineering, Nagoya University
Vol.42, No.1 (1990) −Research Report−

NUMERICAL SOLUTION OF SHOCK TUBE PROBLEM USING FINITE ELEMENT METHOD WITH UPWINDING

S. G. Ravi KUMAUR and Toshi FUJIWARA

Department of Aeronautical Engineering

(Received April 27, 1990)

Abstract

A finite element method is introduced to solve compressible flow problems with discontinuities, using Taylor-Galerkin discretization. A new upwinding parameter is introduced in the calculation of element matrices to resolve the discontinuity and a limiting technique is applied to the derivative of flux to supress numerical oscillations. The adopted technique is used to solve shock tube problems with shock probagation Mach number up to 5. The results are compared with the ones from an upwind TVD explicit scheme and an analytical result. The technique seems to work well for the tested cases as is evident from the presented graphs.

1. Introduction

The immense demand from aerospace industries in the last decade lead to the development of high-resolution non-oscillatory schemes for the prediction of compressible flow fields with strong dicontinuities. High-resolution difference schemes like TVD schemes had been developed and were successfully applied to fluid dynamic and cumbustion problems by Harten[1], Yee[2], Osher and Chakravarthy[3] and others. It had been applied to cumbustion and detonation problems by Yee and Shin[4], Wang and Fujiwara[5] respectively. In finite element context the Taylor-Galerkin method had been used by various researches like Donea[6], Thornton and Ramakrishnan[7] and Selmin[8]. It was applied to chemically reacting flows by Chung and Sohn[9]. All of them made use of different computational strategies to obtain oscillation-free solutions. Donea and others[10] briefed the computational strategies such as two steps for accurate computation, modulated dissipation for oscillation control, and TVD-like limiting procedure for high resolution and non-oscillatory solution. They solved the shock tube problem explained by Sod[11]. They suggested a two-step calculation instead of a single step calculation for accurate results. In the present work a new single-step finite

element procedure using Taylor-Galerkin discretization is tested with upwinding and flux derivative limiting technique. The procedure is used to solve shock propagation problems in a shock tube. The results are compared with the result from an upwind TVD explicit scheme and analytical results.

2. Finite Element Formulation

A system of non-linear hyperbolic equations which represent the compressible, inviscid and unsteady flow can be written as

$$V_t + \nabla . F(V) = 0, \tag{1}$$

where V is the unknown vector and F is the flux vector.
Eq. (1) is discretized in time using Taylor expansion as

$$V^{n+1} = V^n + \triangle t V_t^n + (1/2)\triangle t^2 V_{tt}^n + O[(\triangle t)^3]. \tag{2}$$

Repeated substitution of Eq. (1) in Eq. (2) leads to

$$V^{n+1} = V^n - \triangle t \nabla . F^n - (1/2)\triangle t^2 \nabla . F_t^n, \tag{3}$$

$$V^{n+1} = V^n - \triangle t \nabla . F^n + (1/2)\triangle t^2 \nabla . [A^n \nabla . F^n], \tag{4}$$

where

$$\mathrm{A(V)} = \partial \mathrm{F(V)}/\partial \mathrm{V}.$$

The domain can spatially be discretized into a finite number of elements and the variation of the unknowns can be represented by the interpolation

$$V_e = \textstyle\sum_{i=1,n}^{n} N_i V_i. \tag{5}$$

where N_i is the shape function, and V_i is the set of unknown values associated with a particular node 'i' of an element 'e'. V_e represents the value of the set V at an interior point of the element 'e'. The shape function differs depending on the order of utilized interpolation. In the present study linear interpolation is used.

Applying the Galerkin weighted residual procedure, where the shape functions are substituted for weighting functions, the weak form can be expressed as

$$\begin{aligned} \int_\Omega N_i V^{n+1} d\Omega = \int_\Omega N_i V^n d\Omega - \int_\Omega N_i \{ \triangle t \nabla . F^n \\ - (1/2)\nabla t^2 \nabla . [A^n \nabla . F] \} d\Omega. \end{aligned} \tag{6}$$

Application of Green's theorem and integration by parts will lead to the set of equations

$$\int_{\Omega} N_i[V^{n+1} - V^n]d\Omega = \triangle t \int_{\Omega} \nabla N_i.[F^n - (1/2)\triangle t A^n \nabla . F^n]d\Omega - \triangle t \int_{\Gamma} N_i \vec{n}.[F^n - (1/2)\triangle t A^n \nabla . F^n]d\Gamma. \tag{7}$$

where Ω represents the volume, Γ represents the surface which encloses the volume and $\vec{n}$ represents the unit vector normal to the surface pointing outside.

The general element matrix obtained from Eq. (7) can be represented as

$$[M]_e V_e^{n+1} = [M]_e V_e^n + \triangle t X_e^n, \tag{8a}$$

where V_i is the vector of unknown values at a node 'i',

$$M_{i,j} = \int_{\Omega} N_i N_j d\Omega, \tag{8b}$$

$$X_i = \int_{\Omega} \nabla N_i.\phi_e d\Omega - \int_{\Gamma} N_i \vec{n}.\phi_e d\Gamma, \tag{8c}$$

$$\phi_e^n = F^n - (1/2)\triangle t A^n \nabla . F^n. \tag{8d}$$

The element matrices are assembled into a global matrix and the final set of equations can be written as

$$[\vec{M}]\vec{V}^{n+1} = [\vec{M}]\vec{V}^n + \triangle t \vec{X}^n. \tag{9}$$

The equation corresponding to the node 'i' can be written as

$$\sum_{k=l,m} M_{i,k} V_k^{n+1} = \sum_{k=l,m} M_{i,k} V_k^n + \triangle t \sum_{e=1,l} X_{e,i}, \tag{10}$$

where $X_{e,i}$ is the contribution to the node 'i' from element 'e', 'm' refers to the number of nodes connected to the node 'i', and 'l' refers to the number of elements connected at the node 'i'.

Introduce $\sum_{k=l,m} M_{i,k} V_i^{n+1}$ and $\sum_{k=l,m} M_{i,k} V_i^n$ to the left- and right-hand sides of Eq. (10) respectively. A simple rearrangement will result in

$$\sum_{k=l,m} M_{i,k}(V_k - V_i)^{n+1} + \sum_{k=l,m} M_{i,k} V_i^{n+1} = \sum_{k=l,m} M_{i,k}(V_k - V_i)^n + \sum_{k=l,m} M_{i,k} V_i^n + \triangle t \sum_{e=1,l} X_{e,i}. \tag{11}$$

First-order approximation at any point 'i' can be written as

$$V_i^{n+1} = V_i^n - \triangle t \nabla . F_i^n \tag{12}$$

Substitution of Eq. (12) for the nodes 'i' and 'k' in Eq. (11) and a rearrangement will result in

$$\begin{aligned}&\left[\sum_{k=l,m} M_{i,k}\right](V^{n+1} - V^n)_i \\ &= \triangle t\left[\sum_{e=1,l} X_{e,i} + \sum_{k=l,m} M_{i,k}(\nabla . F_k - \nabla . F_i)\right].\end{aligned} \tag{13}$$

The mass matrix on the left-hand side of the above equation is a lumped one. Hence the described procedure is an explicit one-step scheme, second-order-accurate in time and space, even if linear interpolation is assumed for variables. The described procedure is general and the next section describes the modifications introduced to improve the resolution and supress the numerical oscillations.

3. Techniques Adopted for the Present Solution

The following section describes the upwinding and limiting techniques that were adopted to obtain oscillation-free solutions.

Since the term $\nabla . F_i$ is required for every node in Eq. (13), the following procedure is adopted in evaluating the term. $\nabla . F$ is evaluated in all the elements connected to the node 'i' near the point 'i'. The value of $\nabla . F_i$ is decided from the minmod operation on the values of $\nabla . F$ from all the elements attached to node 'i' like

$$\nabla . F = minmod \nabla . F_{i,e=1,l}. \tag{14}$$

The term X_i in Eq. (8a) consists of the volume and surface integrals of the term ϕ in Eq. (8d). The surface integral of ϕ cancels out after assembly if existence of unique value of $\nabla . F$ is assumed throughout the boundary of integration. The ϕ term in the volume integral is converted into an upwinded numerical flux function like

$$\vec{\phi}_e^{\,n} = F_e^n - (1/2)\alpha_e \nabla t A_e^n \nabla . F_e^n, \tag{15}$$

where α_e is the upwinding parameter evaluated from

$$\alpha_e = 1 + (\chi_{max}/\chi_{min})^{\delta}, \tag{16}$$

where δ can be an any value between 0 and 1. It is observed that δ above 0.5 tends to be more diffusive. The value 0.5 seems to be an optimum one. χ is a property of the flow which varies abruptly, indicating a discontinuity in the flow. In the present case the density is chosen to represent the discontinuity. The volume integral is evaluated numerically using Gaussian quadrature. Next section describes the application of the above-mentioned techniques to the shock propagation problem.

4. Application to Shock Propagation Problem

The finite element procedure described above with the modifications mentioned is applied to shock tube flowfield simulation. The solved system is the Euler equations for a one-dimensional, compressible and inviscid flow represented by Eq. (1) with

$$V = \{\rho, m, e\}^T, \tag{17}$$

$$F = \{m, m^2/\rho + p, (e+p)m/\rho\}^T, \tag{18}$$

$$p = (\gamma - 1)(e - \vec{m}^2/2\rho), \tag{19}$$

where

$$\vec{m} = \rho u,$$

and u is the velocity.

In the present set of numerical experiments, a shock tube of 1 m length is considered. A diaphragm placed at a distance of 0.666 m from the left is assumed to separate the driver section (right) from the driven section (left). The driver gas Helium at high pressure is placed on the right of the diaphragm (0.666 to 1.0 m) and the test gas Argon is placed on the left (0.0 to 0.666 m). At time t = 0 the diaphragm is ruptured and the shock wave propagation starts. The initial pressure ratio between the driver and driven sections is varied for which the numerical results are obtained for the density, pressure, temperature and energy per unit volume. The shock strength, shock Mach number and the Mach number of contact discontinuity are also calculated from the numerical results. They are compared with the analytical results obtained from shock tube equations[12]. The shock Mach number, discontinuity Mach number and the shock strength show a good agreement. Results are also compared with the results from a TVD explicit scheme. The agreement is good as is evident from the presented graphs. The details of the numerical experiments carried out with the present FEM and a TVD method are shown in Figs. 1–4.

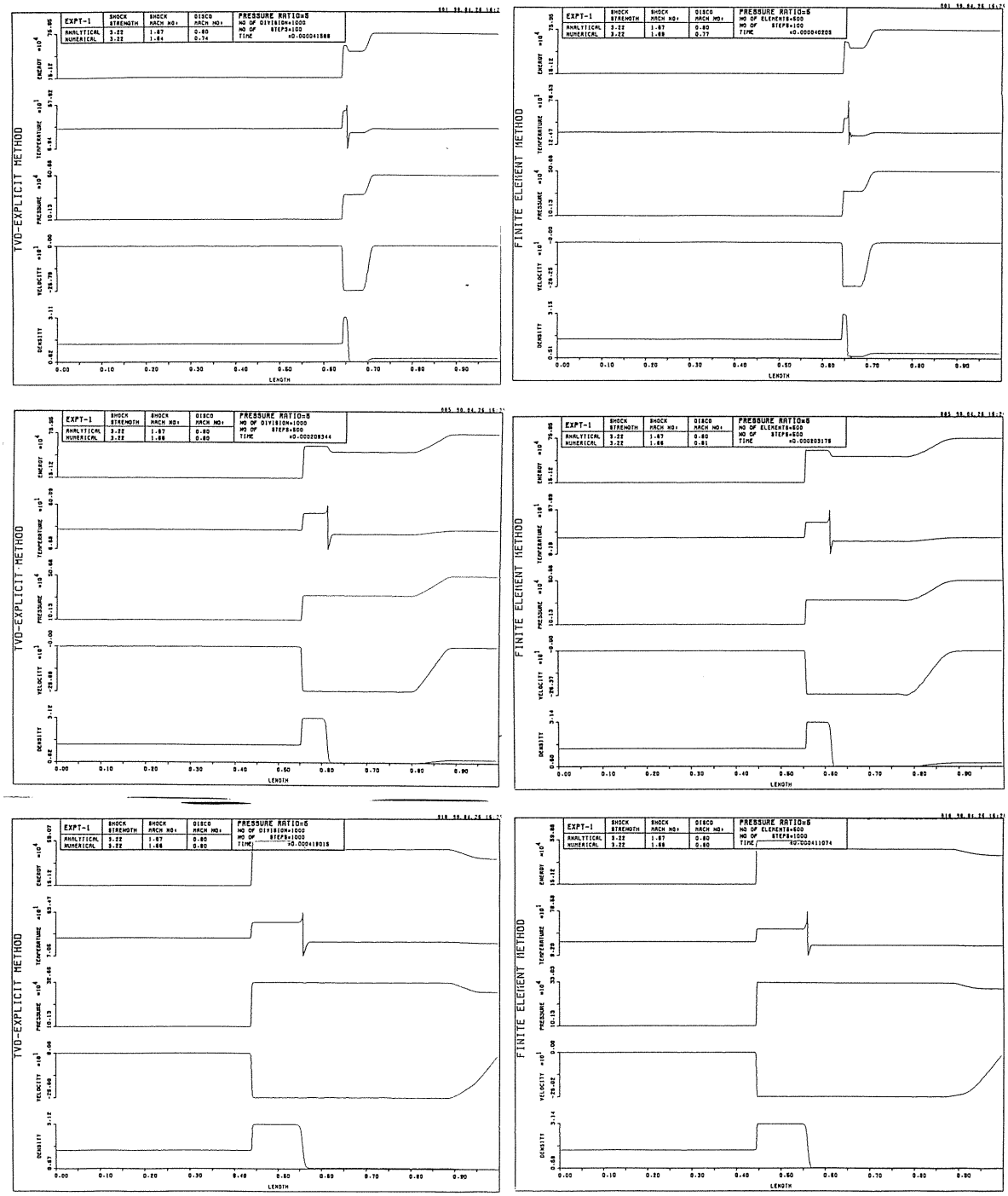

Fig. 1. Results for the case of pressure ratio 5

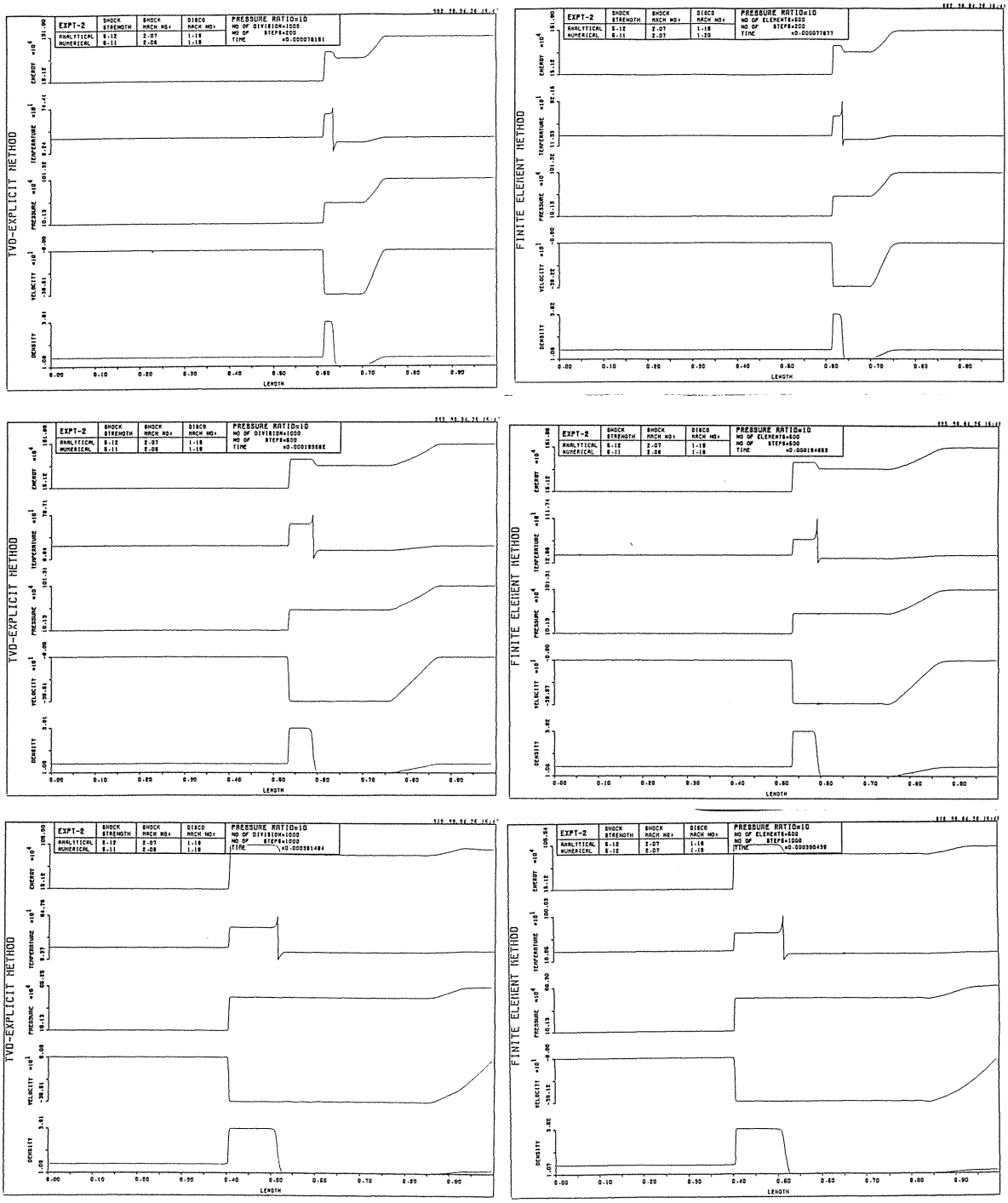

Fig. 2. Results for the case of pressure ratio 10

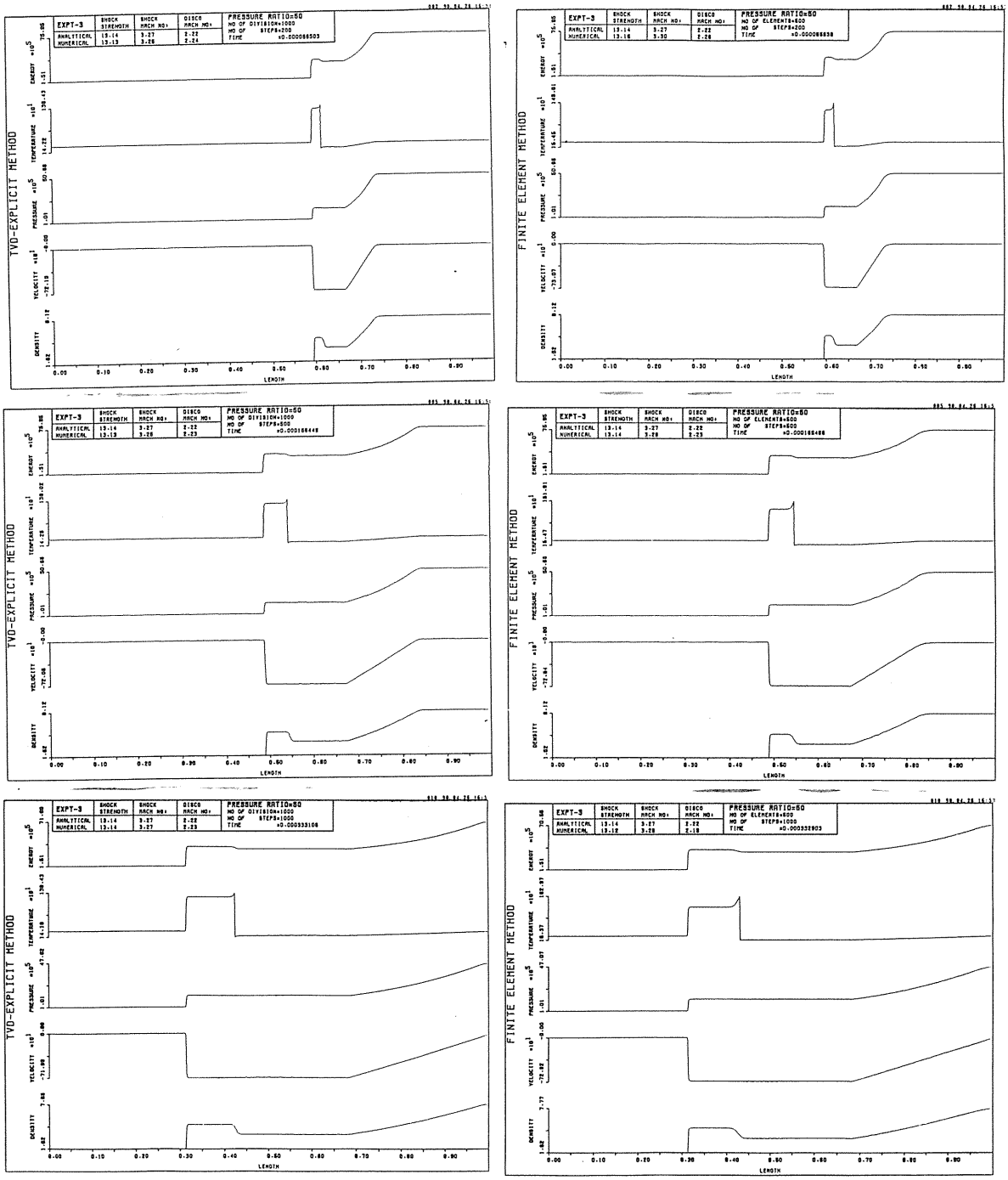

Fig. 3. Results for the case of pressure ratio 50

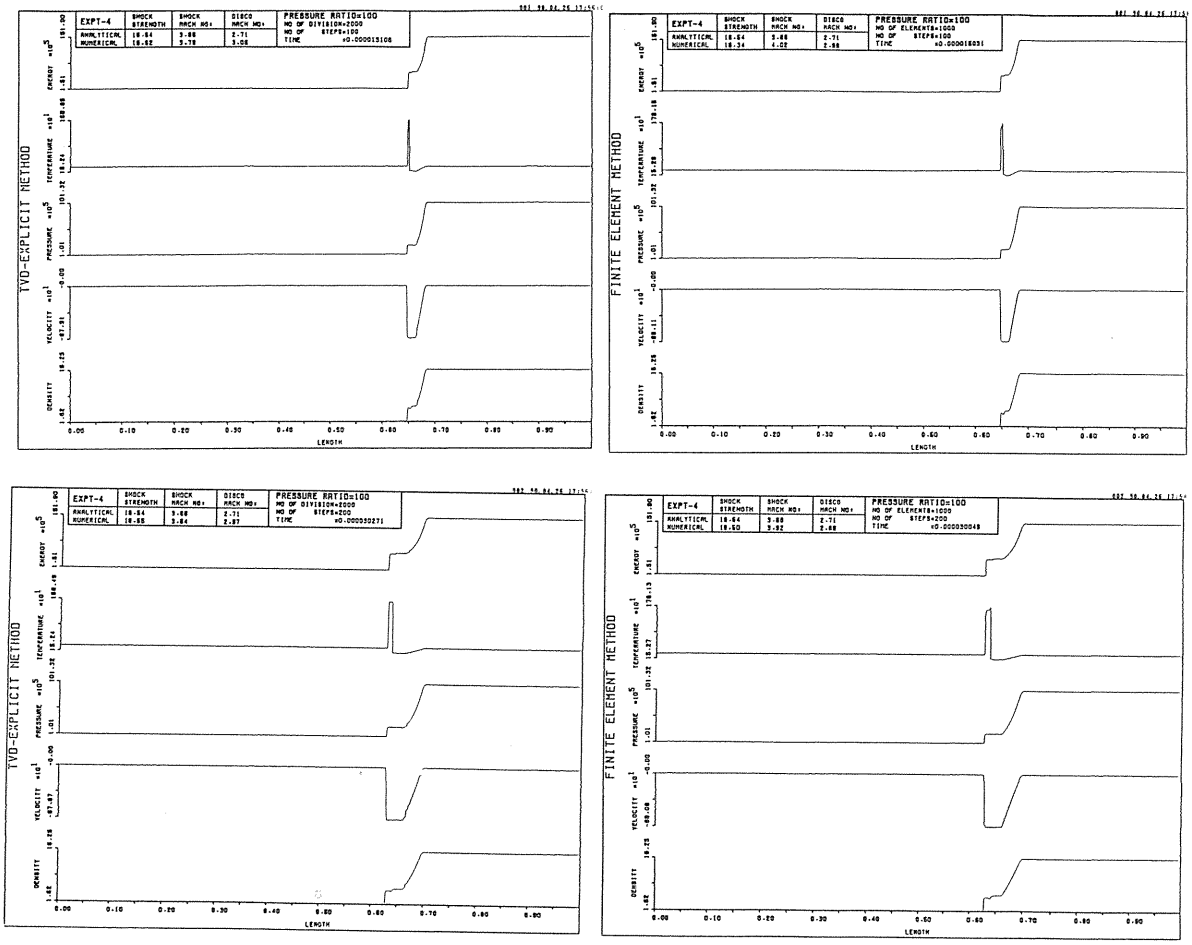

Fig. 4. Results for the case of pressure ratio 100

Four numerical experiments are conducted to the He-Ar system. The driven gas Argon is maintained at the pressure 1 atm and temperature 300°K for all the experiments. The driver gas Helium is initially kept at four different pressures 5, 10, 50 and 100 atm. The initial temperature of Helium is maintained at 300°K for all the experiments.

(i) Discretization details:

In the TVD solution the grid is assumed uniform with total length of 1 m divided into the divisions of equal lengths. In the finite element solution the total length is divided into 3 regions 0.0−0.3 (I), 0.3−0.7 (II) and 0.7−1.0 (III). The individual region is divided further into smaller elements. The element width differs from region to region. In Experiments 1, 2 and 3, the TVD used 1000 grids with constant spacing 0.001, whereas in the finite element calculation the region (I) was divided into 50 elements, the region (II) into 400 elements

and the region (III) into 50 elements. In Experiment 4 the TVD scheme utilized 2000 grids with spacing 0.0005. In the finite element method the region (I) into 100 elements, the region (II) into 800 elements and the region (III) into 100 elements. The mesh resolution in the region (II) of the finite element method is equal to that of the TVD scheme. Hence the results from the two methods can be compared directly. Varying the grid size in the present experiment also demonstrates the selective mesh refinement technique. Since the transient solutions are compared only for a short time, the shock wave does not get out from the region (II). If shock reflection has to be studied, then the grid can be redefined when the shock is just about crossing the region (II).

(ii) Courant number:

Courant number in both methods is kept at 0.5 for all the experiments. The present method gave stable results up to Courant number 0.8.

(iii) Results:

Numerical results are presented in graphical forms. Since the problems are transient in nature, the results at 3 different times are shown. The results from an explicit TVD scheme for the same problems are also presented in the same scale for comparison. The numerical values of Mach number and shock strength calculated at that instant are shown in the graphs along with analytical results. The results show a good agreement with the analytical results and the TVD results. Even though small undershoots near the shock wave are observed during the initial development of shock, it is reduced as the shock propagates. This shows that the present scheme has a good convergence property. The discontinuities are traced after every time step. Since the used algorithm suffers from some Gibbs phenomena, the exact location of the discontinuities becomes difficult in some cases where reversal of gradient occurs frequently near the discontinuities. Hence, the numerical values are not exactly agreeing with the analytical results. But the accuracy on the prediction of discontinuity location seems to be satisfactory.

5. Conclusions

The results from the present method show a high resolution, without deteriorating numerical oscillations, comparable to the TVD scheme. Further investigation of the advantage and shortcomings of the method is under investigation.

References

1) A. Harten, Journal of Computational Physics. **49** (1983), 357.
2) H.C. Yee, NASA Technical memorandum 89464, May 1985.
3) C.R. Chakravarthy and S. Osher, AIAA paper 85-0363, Jan. 1985.
4) J.L. Shinn and H.C. Yee, AIAA paper 87-1577, June 1987.
5) Yi-yun Wang and T. Fujiwara, AIAA paper 88-0478, Jan. 1988.
6) J. Donea, L. Quartapelle and V. Selmin, Journal of Computational physics. **70** (1987), 463.
7) E.A. Thornton and R. Ramakrishnan, Fifth International Symposium on Finite elements and flow problems, Eds G.F. Carey and J.T. Oden Austin, Texas, 1984.

8) V. Selmin and L. Quartapelle, Proceedings of the Tenth international conference on Numerical Methods in Fluid Dynamics, Beiing, China, June 1986.
9) T.J. Chung, Y.M. Kim and J.L. Sohn, International Journal of Numerical method in Fluids. **7** (1987), 989.
10) J. Donea, L. Quartapelle and V. Selmin, Numerical methods for fluid dynamics III. Eds, K.W. Morton and M.J. Baines, Oxford Science publication, 1988.
11) G.A. Sod, Journal of Computational Physics. **27** (1978), 1.
12) H.W. Liepmann and A. Roshko, Elements of Gas Dynamics, Joh Wiley and Sons Inc. 1957.